Modernization of the Installation for Production of Nanopowders of Metal Oxides Using Pulsed Electron Beam

V.G. Il'ves, A.S. Kamenetskikh, Yu.A. Kotov, S.Yu. Sokovnin, and A.I. Medvedev

Institute of Electrophysics UB RAS, 106, Amundsen str., Ekaterinburg, 620216, Russia
E-mail: sokovnin@iep.uran.ru

Abstract – Considering the obtained results, we developed and make up a modernization of the installation for production of nanopowders of metal oxides. A method for production of nanopowders, including evaporation of a target by a pulsed electron beam, condensation of the vapor of the material in a low-pressure gas, and deposition of nanopowders on a cold big square crystallizer.

The installation for realization of the method consists of a pulsed electron beam source, a beam guidance and focusing system, a gas pressure differential system, an evaporation chamber, a target, and a powder collecting system, which is a coreless cylinder that cooled on the inside.

The use of more powerful hollow-cathode gas-filled diode allows forming up to 1 A electron beam with 100 μs pulse length. Big diameter (0.3 m) and length (0.5 m) cooling cylinder allow having low agglomerated nanopowders.

The results of evaporated targets from YSZ and $CeGdO_x$ were achieved.

By this method, it is possible to produce nanopowders of the oxide with the characteristic size of 3–5 nm and nanopowder agglomerates with the characteristic size of 20–200 nm having the specific surface of up to 250 m^2/g at the production rate of up to 10 g/h and the specific energy consumption of less than 120 W · h/g.

1. Introduction

Many problems are solved successfully by nanopowder production methods envisaging pulsed heating and evaporation of targets, e.g., by application of a current pulse for electrical explosion of wire (EEW) [1] or irradiation from a pulsed CO_2 laser [2]. These methods have advantages and disadvantages. The use of a pulsed electron beam for evaporation of targets solves the problems encountered in the said methods as regards a higher efficiency of the energy to radiation conversion in comparison with laser and making of targets from inexpensive materials of different compositions for productivity compound materials in comparison with EEW.

The "Nanobeam-1" installation, which was developed for production of nanopowders by evaporation of targets by pulsed electron beams, condensation of the vapor of the material in a low-pressure gas and deposition of nanopowders on a cold crystallizer, demonstrated practicability as well as certain advantages and disadvantages of the method [3]. The accumulated experience has led to development of a modernized "Nanobeam-2" installation.

2. Installation description

The block diagram of the installation is shown in Fig. 1 and its technical characteristics are given in Table 1.

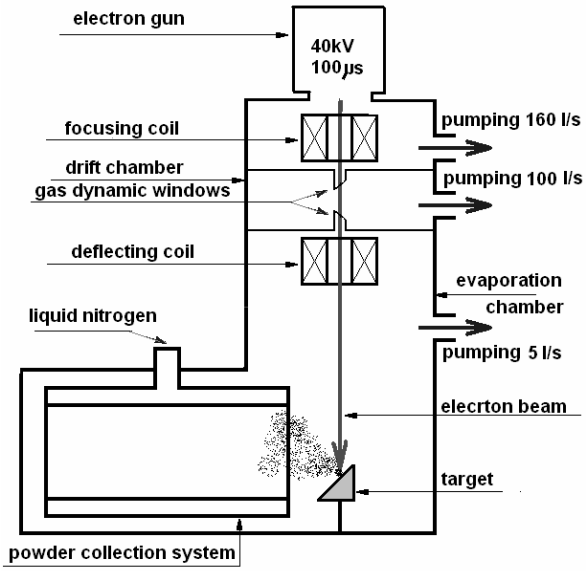

Fig. 1. Block diagram of the "Nanobeam-2" installation

Table 1. Technical characteristics of the "Nanobeam-2" installation

No.	Characteristics	Value
1	Power consumption, kV · A, maximum	5
2	Power mains	380 V (3 phases), 50 Hz
3	Pulse length, μm	50–100
4	Pulse repetition rate, Hz	up to 500
5	Accelerating voltage, kV	up to 40
6	Beam current at the target, A	0.6
7	Beam diameter at the target, mm	1.5
8	Adjustment range of the evaporation chamber pressure, Pa	10^{-1}–10^5
9	Rate of the gas inleakage to the evaporation chamber, l/h	up to 63
10	Weight of the installation, kg, maximum	700
11	Installation floor area, m×m	3×3

The electron gun requires a pressure of about 10^{-2} Pa for its normal operation, while a high pressure is desirable in the evaporation chamber for quick cooling of particles. These contradictory requirements are satisfied by pumping from three zones, which are separated by two gas dynamic windows with holes of diameter 3.2 mm spaced a distance of 100 mm from one the other in the drift chamber with the focusing and deflecting coils.

Air is pumped from the electron gun and drift chambers by AVDM 160 and AVDM 100 pump units respectively, while from the evaporation chamber by a 2NVR-60D pump.

All the chambers are made of stainless steel and are coated on the outside with lead plates 5 mm thick for protection against bremsstrahlung. The peepholes are protected with lead glass 20 mm thick.

The operating experience with the "Nanobeam" installation demonstrated that the electron gun [4] provided an insufficient current amplitude and, thus, the pulse duration had to be increased for accumulation of the required energy that had increased the energy losses by means of thermal conductivity. For this reason, a new electron gun with a plasma emitter, which generates a pulsed electron beam with the pulse repetition frequency of 1–500 Hz and the current pulse length of 100 μs, has been designed. The gun relies in its operation on a glow discharge initiated in cylindrical hollow cathode *1* (Fig. 2) of internal diameter 15 mm and 20 mm high.

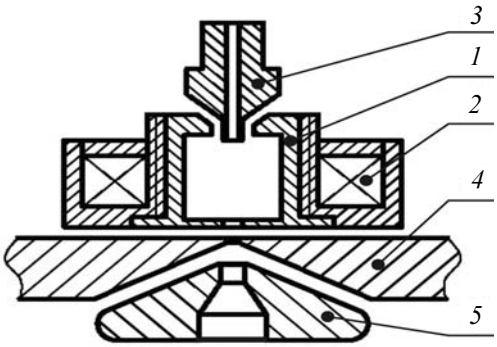

Fig. 2. Gas-discharge system of the electron source: *1* – hollow cathode; *2* – magnet; *3* – ignitor electrode; *4* – anode; *5* – accelerating electrode

The ring magnet generating a 0.1 mT field on the axis is mounted externally on the hollow cathode. The gas is leaked into the hollow cathode through a channel in ignitor electrode *3*. Anode *4* is installed opposite the exit hole of diameter 3 mm in the hollow cathode. As distinct from [4], the diameter of the exit aperture is smaller than the internal diameter of the hollow cathode, reducing the electron loss area. A high voltage (up to 40 kV), which ensures extraction of electrons from the plasma through an emission orifice of diameter 1.2 mm and the formation of a beam with a current of up to 1 A, is applied between the anode and accelerating electrode *5*.

The beam is scanned on the target continuously similarly to the TV scan, while the scan area can be adjusted between 0.8 and 4 cm^2.

The target (a pellet 40/60 mm in diameter and up to 20 mm high) is placed in a support capable of moving freely (with locks) in two planes. The target is installed horizontally for alignment and focusing of the electron beam. For evaporation, the target is tilted at an angle of 45° to the beam toward the crystallizer so as to increase the powder collection. By design, the support allows rotating the target at a speed of 8.7 rpm for more uniform evaporation and permits moving the target away from the edge of the deflecting coil to a distance of 80 to 170 mm.

The powder collection system [3] employing a cooled revolving hollow disk proved to be inconvenient in operation. Moreover, the proportion of the collected powder considerably decreased for geometrical reasons with increasing distance between the target and the disk. Now the modernized powder collection system includes a hollow copper cylinder of the internal diameter 300 mm, which is installed at the right angle to the beam axis at a distance of 7 mm from the edge of the target. The cylinder is cooled on the inside with liquid nitrogen supplied at a rate of about 5 kg/h. The powder is collected from the cylinder by a scraper. To facilitate the collection process, the surface of the cylinder is covered with a stainless steel sheet (0.8 mm thick) having a polished surface.

The following methods were used for examination of the materials:

– the specific surface of the powders S_s was measured by the BET method on a TriStar 3000 V6.03 analyzer;

– the chemical composition of the powders was determined and the X-ray diffraction analysis was performed using standard methods on a D8 Discover X-ray diffractometer;

– the microscopic analysis was made in LEO-982 and JEOL 2100 scanning electron microscopes.

The accelerating voltage of 37–40 kV was used in the experiments. Upon transportation and focusing the beam current on the target was not less than 0.46 A at the beam diameter of about 1.00 mm, providing the power density (the intensity) of about $3 \cdot 10^6$ W/cm^2.

The pressure of the evaporation chamber was adjusted between 3.8 and 50 Pa. The beam energy loss caused by this adjustment was several percent and was disregarded. Air, oxygen and argon were used in the experiments and the gas inleakage rate was controlled by RMK rotameters (GOST 13045).

The total current of the electron beam and the beam current hitting the target were measured by current transformers (CT) installed in the accelerating voltage source and on the target support acting as a current lead. The shunt in the connection between the upper gas dynamic window and the casing allowed measuring the proportion of the current lost as the beam was transported through the window.

The operating principle of the device is as follows. The electron beam is focused at the hole of the upper gas dynamic window and, as is passes through the second gas dynamic window, is focused additionally by the deflecting coil. This coil also sweeps the beam on the target. The material of the target evaporates under the action of the beam; the vapor-plasma mixture is cooled by the low-pressure gas in the evaporation chamber; and the vapor condenses with the formation of nanopowder particles. The powder flies to the cooled crystallizer and is deposited thereon.

The following oxides were used for making of powders in the experiments: 10 YSZ (zirconium stabilized with 10 molar % of yttrium) and $Ce_{1-x}Gd_xO_{1-\delta}$ (gadolinium-doped ceria).

The synthesized YSZ powders had a large specific surface and were agglomerated to complexes 5 to 600 nm in size, which consisted of particles with a sufficiently narrow size distribution of about several nm (Fig. 3). The specific surface of the synthesized YSZ powders could be as large as S_s = 250 m^2/g.

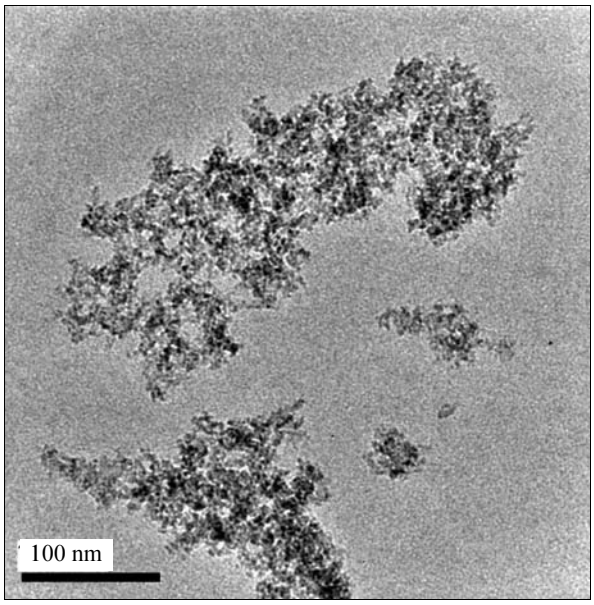

Fig. 3. TEM photographs of a 10 YSZ powder

The X-ray diffraction analysis of the synthesized powder showed that the sample had two phases. The first phase was a solid solution of Y_2O_3 in the cubic modification of ZrO_2. The lattice spacing a = 5.148 Å and the coherent scattering regions (CSR) were 130 nm in size. The Y_2O_3 concentration was ≈ 11 mole %. The varying concentration of yttrium, relative to the target, suggested that the phase was not fragments of the target, but represented a synthesis product. The concentration of this phase was ≈ 7 weight %. The second phase (≈ 93 weight %) was an X-ray amorphous phase with the short-range order characteristic of the monoclinic form of zirconia. The CSR was 1÷2 nm in size on the average.

The obtained result is nontrivial. Earlier investigations into synthesis of zirconium nanopowders (our data and the literature [5]) showed that the tetragonal and cubic phases, which are most metastable at room temperature, are stabilized with decreasing size of the particles. In this experiment, the finest phase is the monoclinic one, i.e., the most stable phase. This would not be so if pure zirconium were synthesized. We synthesized yttrium-stabilized ZrO_2. The stable phase for this compound is the cubic modification. The most metastable is the monoclinic phase and, naturally, it is this phase that forms in finest particles.

The experiments with gadolinium-doped ceria confirmed the earlier results and demonstrated the possibility of producing powders with S_s of about 190 m^2/g. The synthesized powders had a large specific surface and were agglomerated to complexes 20 to 600 nm in size similar to those of YSZ (Fig. 4).

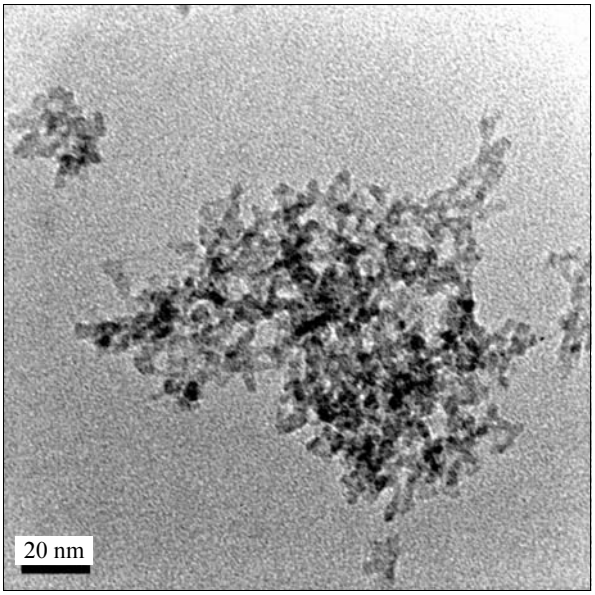

Fig. 4. Photographs of $Ce_{1-x}Gd_xO_{1-\delta}$ powders

The X-ray diffraction analysis showed that two phases – a mechanical mixture of CeO_2 and Gd_2O_3.

Given below are characteristics of their structures.

CeO_2: a cubic lattice of the fluorite type with the spacing a = 5.413 Å; the CSR 84 nm in size; and the concentration of ≈ 82 weight %;

Gd_2O_3: a cubic lattice of the Mn_2O_3 type with the spacing a = 10.89 Å; the CSR 124 nm in size; and the concentration of ≈ 18 weight %.

Remarkably, the value of the lattice spacing of the phase at hand is considerably different from the corresponding values reported in the literature (10.797 ÷ 10.813 Å).

The difractogram of nanopowders was complex and has not simple interpretation. Two phases model is the most convenient – both phases were the solid solution Gd_2O_3 in a cubic lattice of the CeO_2. The phases have the different size of CSR and chemistry (the various content of gadolinium).

In Fig. 5 is shown the results of more accurate definition of difractogram using the method of fullpro-

file analysis was calculated such characteristics of the structures:

– fine-crystalline phase: the average dimension of the CSR ≈ 3.5 nm, a cubic lattice spacing a = = (5.43 ± 0.01) Å, the concentration of ≈ 97%.

– "macrocrystalline" phase: the average dimension of the CSR ≈ 40 nm, a cubic lattice spacing a = = (5.420 ± 0.003) Å, the concentration of ≈ 3%.

Thus, both in YSZ and in gadolinium-doped ceria systems the two phase's material is synthesized independent on the targets structure was: a one phase solid solution (as YSZ) or a mechanical mixture of components. The forming in the synthesizing process two phases with the different size of the CSR and chemistry is of fundamental importance and is special for our method.

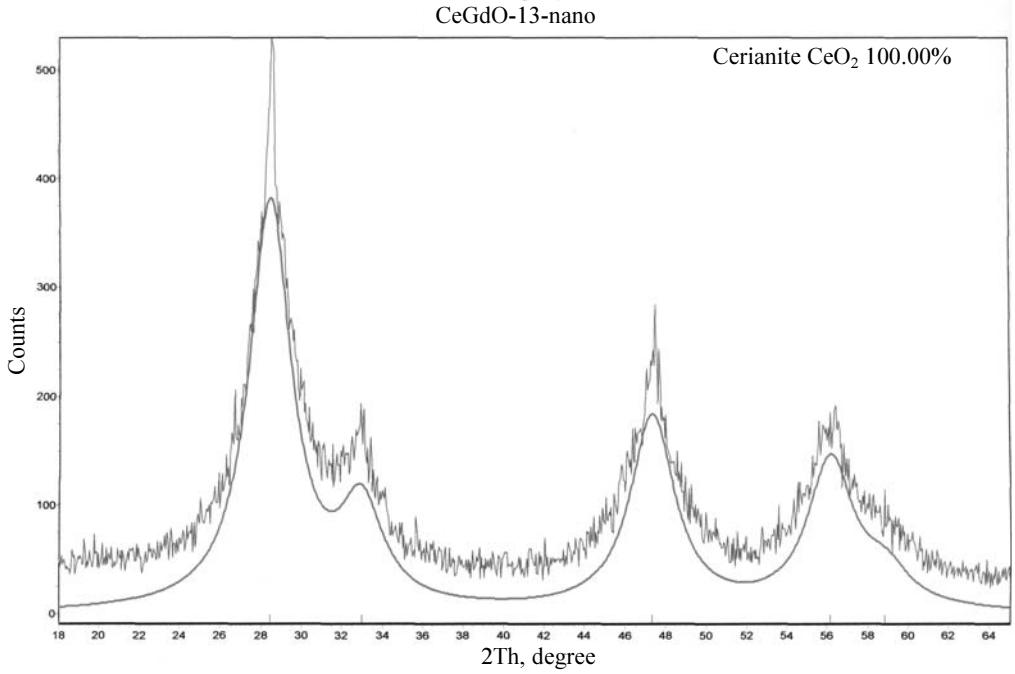

Fig. 5. Diffraction pattern of the target ($Ce_{1-x}Gd_xO_{1-\delta}$)

3. Conclusion

The modernized installation considerably improves parameters of the synthesized powders and is more convenient to operate. The electrode system of the new electron gun is designed such as to ensure its more reliable operation in dust-laden conditions, which are inevitable for this installation. The installation allows making agglomerates of oxide nanopowders with S_s of up to 250 m^2/g at the output capacity of up to 12 g/h and the specific energy consumption of $W_3 > 112$ kW · h/g (nearly 5 sublimation energies).

The powder agglomeration can be avoided and the loss of the material can be reduced by provision of the largest possible distance between the target and the powder collection system, which should receive the largest possible flow of the vapor-plasma cloud. That is, it is reasonable to change to the 4π geometry: the installation of crystallizers on both sides of the target.

Acknowledgements

The authors wish to thank T.M. Demina, who measured the specific surface of the powders, A.M. Murzakayev for the electron microscopic examination of the samples.

References

[1] Yu.A. Kotov, J. of Nanoparticle Res. **5**, 539 (2003).
[2] Yu.A. Kotov, V.V. Osipov, O.M. Samatov et al., ZhTF **74**, 72 (2004).
[3] V.G. Ilves, Ya.A. Kotov, S.Yu. Sokovnin, and C.K. Rhee, Rossijskie Nanotekhnologii **2**, 96 (2007).
[4] V.V. Ilyushenko and N.G. Rempe, Prib. Tekh. Eksper. **4**, 73 (1994).
[5] Yu.A. Kotov, V.V. Osipov, O.M. Samatov et al., *in Pros. V All-Russian Conf. Physics of superdispersed systems*, Part 1, Ekaterinburg, 2001, pp. 69–77.